REVISTA INTERDISCIPLINAR DE PESQUISA EM ENGENHARIA

CILAMCE 2016
XXXVII IBERIAN LATIN AMERICAN CONGRESS ON COMPUTATIONAL METHODS IN ENGINEERING
BRASÍLIA - DF - BRAZIL

DEVELOPMENT OF A COMPUTER CODE USING THE LAGRANGIAN SMOOTHED PARTICLE HYDRODYNAMICS (SPH) METHOD FOR SOLUTION OF PROBLEMS IN FLUID DYNAMICS AND HEAT TRANSFER

Carlos Alberto Dutra Fraga Filho

cadff1@gmail.com

Federal Institute of Education, Science and Technology of Espírito Santo – Engineering Mechanical Coordination – Av. Vitória, 1729 – 29040-620 – Jucutuquara – Vitória – ES – Brazil

Abstract. The Lagrangian Meshless Smoothed Particle Hydrodynamics (SPH) method is an alternative to the traditional mesh Eulerian methods for solving engineering problems. Although it began to be used a few decades ago, SPH method has advantages compared to methods with meshes, in the numerical solution of classical problems studied in engineering courses. The numerical SPH method allows a better visualisation of the spatio-temporal evolution of the flow (and the fluid properties), and a lower computational cost in the study of complex geometries with topological changes or free surfaces, providing stable numerical solutions. There has been an increase in the applications of particle methods in Computational Fluid Dynamics (CFD) courses, in the area of fluids and thermal sciences. A computer code has been developed and implemented using FORTRAN Programming Language. Three classical engineering problems have been simulated: diffusion in a flat plate, still fluid within an immobile reservoir and dam breaking. In code validation, numerical results obtained showed a good agreement with the analytical and experimental results reported in the literature. The numerical code developed and presented in this work, is a valuable tool for the teaching of CDF in engineering courses.

Keywords: *CFD education, Computer code, Smoothed Particle Hydrodynamics method, SPH, Meshless method, Engineering courses.*

1 INTRODUCTION

The Eulerian view is historically the most commonly used in modelling of physical problems involving fluids. This modelling requires the use of numerical methods employing grids or meshes, such as finite differences (FDM), finite volumes (FVM) and finite elements (FEM), for the solution of partial differential equations (PDEs) or integral formulations (Liu & Liu, 2010). Based on an adequately meshed preset, the governing equations can be converted to a set of algebraic equations with nodal unknowns for the field variables. However, these Eulerian methods have limitations for applications in various types of complex problems.

The greatest difficulties in using meshes are in ensuring consistence. Employing meshes can lead to a number of difficulties when dealing with fluid flow problems with free surface, mobile interfaces, complex geometries and topological changes. If there are these features, generation of a mesh, a prerequisite for the numerical simulation of quality, is a difficult process, both time-consuming and expensive.

Lagrangian modelling is based on the hypothesis that the problem domain can be divided into a finite number of particles that do not interact with one another. Each particle receives the coordinates that define its position in space; the physical properties of each Lagrangian element are found at each instance in time.

The Lagrangian particle model is meshless and has been an alternative applied in research, pointing to the use of more effective computational methods for solving complex problems, providing stable and accurate numerical solutions for PDEs or integral equations. Some of the advantages of the use of Lagrangian modelling regarding the Eulerian are the simplicity and lower computational cost in complex geometries, not needing the use of meshes, non-production of numerical oscillations, conservation of mass at the Lagrangian element, and finally the graphical visualisation of the results to allow for better understanding of the spatio-temporal evolution of the flow.

Until a few decades ago, Lagrangian modelling has not been used in mathematical-numerical modelling problems in Fluid Mechanics. Fox & McDonald (1988) reported that describing the movements of individual particles would be impractical, employing another type of description for the fluids being more convenient. For a long time, Lagrangian modelling was put aside in favour of Eulerian methods.

One of the critical points of particle models is the processing time: in general, higher than that required by mesh methods. However, the progress of the processing techniques, the rapid spread of multi-core processors, and parallelisation, made possible the use of particle methods, without any viability in problems of fluid mechanics until some years ago. Currently, parallelisation of the graphics processing units (GPUs), using Compute Unified Device Architecture (CUDA), developed by NVIDIA, allows the use of more than one million particles in the discretisation of the fluid domain (Crespo et al., 2011).

The remainder of this article is organised as follows. In Section 2, methodology for the analysis of a physical problem in CFD is presented. The fundamentals of the SPH method are in Section 3. In Section 4, the computer code developed is presented. The validation of the computer code (with numerical simulations performed and results analysis) is shown in Section 5. Finally, the conclusions are presented in Section 6.

2 PHYSICAL PROBLEM ANALYSIS METHODOLOGY

To obtain the solution of any physical problem in Computational Fluid Dynamics, the researcher/ programmer should go through the following steps: observation and understanding of the physical problem; development or use of a mathematical model able to describe it; choice of a numerical method capable of properly solving the equations of the mathematical model, with consistency, speed and accuracy; implementation or use of an existing numerical code to perform the numerical simulations; and, finally, the analysis of the results from the computer simulations. Figure 1 shows these steps in a flowchart.

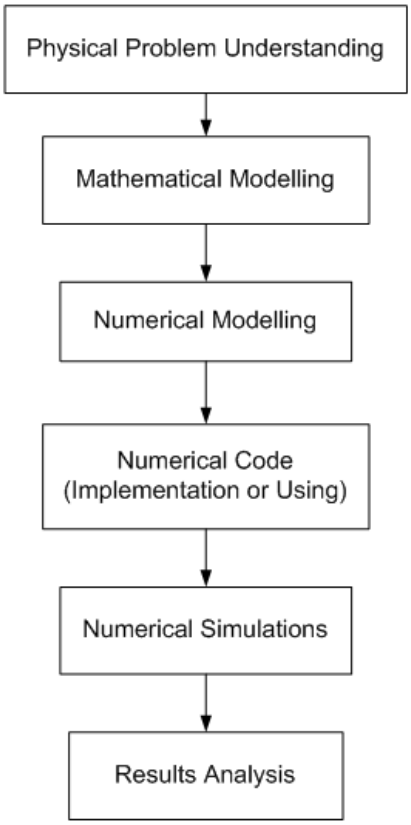

Figure 1. Procedure for numerical simulation of a physical problem.

With specific regard to the choice of numerical method to be employed in the solution of Fluid Mechanics problems, SPH is increasingly used for the following reasons:

- Free surfaces, interfaces and mobile boundaries can be naturally traced by particles in the simulation process;
- Ease of capturing the free surfaces and their topological changes;
- No need for remeshing (one characteristic of mesh methods) at each numerical iteration, which decreases the computational cost in the remeshing operations;
- Conservation of mass for each Lagrangian element (particle);
- The particles' history can be easily obtained, and their visualisation is available, allowing for a better understanding of the phenomenon through time;
- Control of undesirable numerical diffusion, a characteristic problem of methods based on meshes.

3 SPH METHOD FUNDAMENTALS

SPH is based on the valid mathematical identity for a scalar function $f(\boldsymbol{X})$, defined and continuous over the whole domain:

$$f(\boldsymbol{X}) = \int f(\boldsymbol{X}')(\boldsymbol{X}' - \boldsymbol{X})\, dX' \tag{1}$$

where

$f(\boldsymbol{X})$ is a scalar function defined at the fixed point $\boldsymbol{X} = (\mathrm{x}, \mathrm{y})$,

$\delta(\boldsymbol{X}' - \boldsymbol{X})$ is the Dirac Delta function:

$$\delta(\boldsymbol{X}' - \boldsymbol{X}) = \begin{cases} 1, & \text{if} \quad \boldsymbol{X} = \boldsymbol{X}', \\ 0, & \text{if} \quad \boldsymbol{X} \neq \boldsymbol{X}' . \end{cases}$$

By replacing the Dirac Delta function with the smoothing function, W, the approximation to the function at position X is obtained:

$$f(\boldsymbol{X}) = \int f(\boldsymbol{X}') W(\boldsymbol{X}' - \boldsymbol{X}, h)\, dX' \tag{2}$$

where

h is the support radius,

$dX' = d\mathrm{x}'\, d\mathrm{y}'$ is the infinitesimal area element.

The essence of the SPH method is in the discretisation of the domain, Ω, in a finite number of particles and in these Lagrangian elements to obtain the values of the physical properties through from weighted interpolations, from the properties of the particles in the vicinity. Only the neighbouring particles, which are within the influence domain (at a maximum distance kh of the fixed particle considered, k being a scale factor that depends on the kernel employed), contribute to its behaviour.

For the solutions obtained in the interpolations to be representative of the domain of the problem, the number of neighbouring particles within the influence domain must be five, 21 and 57 in 1D, 2D and 3D cases, respectively (Liu & Liu, 2003). Figure 2 shows the arrangement of particles within the influence domain.

Searching for the neighbouring particles can be performed directly or using grids, which leads to a lower number of mathematical operations and reduces the computational cost (Liu & Liu, 2003; Gesteira et al., 2010). Figure 3 shows the direct search (in which all pairs of particles "ab" at the domain will have the distances calculated and compared to the kh value) and the use of a grid, which reduces the number of searching operations (only particles within the shaded region, with three, nine or 27 cells, in 1D, 2D or 3D cases, respectively, will be verified, whether or not they neighbour a reference particle).

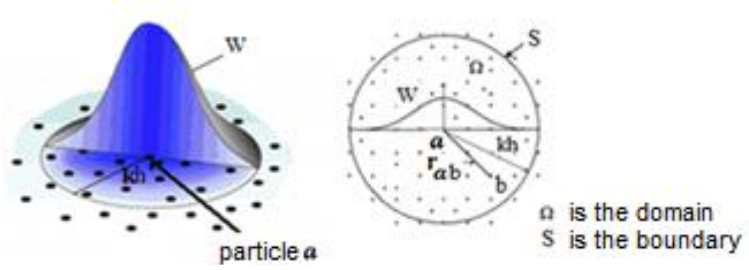

Figure 2. Graphical representation of the influence domain. (a) The reference (fixed) particle, a, has neighbouring particles (b) within the influence domain. (b) The kernel (W) ensures a greater contribution from the nearest neighbouring particles for the value of the physical property in the reference particle.

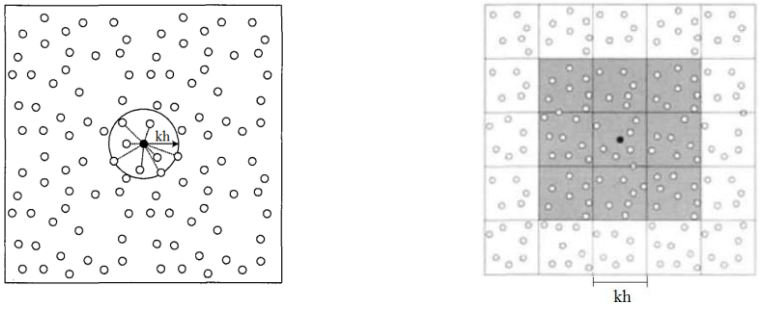

(a) (b)

Figure 3. Neighbouring particles search. (a) Directly. (b) Using a grid (Adapted from: Liu & Liu, 2003).

Different kernels can be used, and so that they are considered suitable for interpolation, it is necessary that each one follow certain properties: smoothness, positivity, symmetry, convergence, decay, compact support, and normalisation within the domain of influence. The cubic spline kernel, proposed by Liu & Liu (2003), is presented in Eq. (3). This smoothing function and its derivatives have a desired mathematical behaviour, favourable for the representation of the physical properties studied.

$$W(r,h) = factor \begin{cases} \left(\frac{2}{3} - q^2 + \frac{1}{2}q^3\right), & 0 \le q \le h \\ \left[\frac{1}{6}\left(2 - q^3\right)\right], & h < q \le 2h \\ 0, & \text{in other case.} \end{cases} \tag{3}$$

where

X_a and X_b are the positions of the fixed and neighbouring particles, respectively.

$q = |X_a - X_b|$,

$$factor = \begin{cases} \frac{15}{7\pi h^2}, & \text{in } 2\text{D}, \\ \frac{15}{\pi h^3}, & \text{in } 3\text{D}. \end{cases}$$

Other kernels are used in the SPH method: quartic proposed (Lucy, 1977); quintic (Gesteira et al., 2010); quintic spline (Morris, 1997); new quartic (Liu & Liu, 2003), each being recommended for the study of a particular physical problem. Figure 4 shows the kernel used by Lucy (1977) in his pioneering work, and the cubic spline employed here.

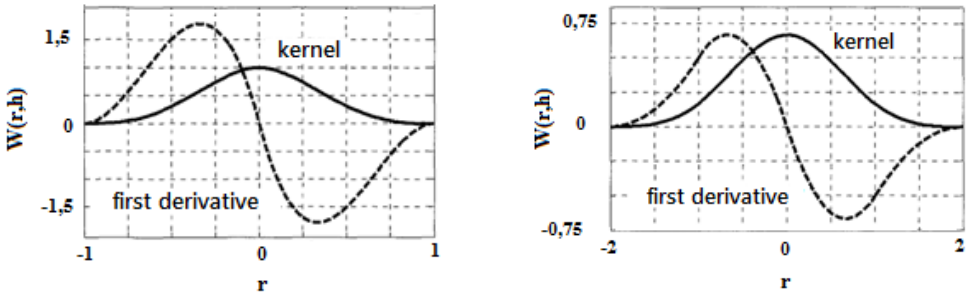

(a) (b)

Figure 4. Kernels and their first-order derivatives. (a) Lucy's (1977) kernel and (b) Cubic spline, used here. Adapted from Liu & Liu (2003).

SPH approaches physical properties (such as density), gradients (pressure gradients), divergence (velocity divergence) and Laplacians (temperature and velocity Laplacians) related to fluid flow, with a second-order error.

The general equation for the approximation of a scalar physical property of a fixed particle a is:

$$A_a = \sum_{b=1}^{n} m_b \frac{A_b}{\rho_b} W\left(\boldsymbol{X}_a - \boldsymbol{X}_b, h\right) \tag{4}$$

For the divergence of a vectorial physical property, the following form can be used:

$$\nabla . \boldsymbol{A}_a = \frac{1}{\rho_a} \sum_{b=1}^{n} m_b \left(\boldsymbol{A}_b - \boldsymbol{A}_a\right) . \nabla W\left(\boldsymbol{X}_a - \boldsymbol{X}_b, h\right) \tag{5}$$

For gradient of A_a (symmetric form):

$$\nabla A_a = -\rho_a \sum_{b=1}^{n} m_b \left(\frac{A_a}{\rho_a^2} + \frac{A_b}{\rho_b^2}\right) \nabla W\left(\boldsymbol{X}_a - \boldsymbol{X}_b, h\right) \tag{6}$$

The following expression can be used for the Laplacian approximation of a scalar property (Fraga Filho & Chacaltana, 2014):

$$\nabla^2 A_a = 2 \sum_{b=1}^{n} \frac{m_b}{\rho_b} \left(A_a - A_b\right) \frac{\boldsymbol{X}_a - \boldsymbol{X}_b}{\left|X_a - X_b\right|^2} . \nabla W\left(\boldsymbol{X}_a - \boldsymbol{X}_b, h\right) \tag{7}$$

where

∇ is the mathematical vector operator nabla;

$\boldsymbol{X}_a$ is the position of the particle a;

$\boldsymbol{X}_b$ is the position of the particle b;

A_a is the scalar physical property approximated by the fixed particle a;

A_b is the scalar physical property of the neighbouring particle b;

$\boldsymbol{A}_a$ is the vector physical property of the reference particle;

$\boldsymbol{A}_b$ is the vector physical property of the neighbouring particle b;

n is the number of neighbouring particles within the influence domain;

m_b is the mass of particle b;

W is the kernel;

h is the support radius;

ρ_b is the density of the neighbouring particle b.

In the SPH method, created for the simulation of compressible fluid, the pressure is an explicit function of the local density of the fluid. In the dynamic case, the compressible fluid is approximate to an incompressible fluid through a quasi-compressible fluid, and pressure is calculated by an equation of state. The Tait Equation is commonly used (as used here) to predict the dynamic pressure (Batchelor, 2000):

$$P_{dyn(a)} = B\left(\left(\frac{\rho_a}{\rho_0}\right)^{\gamma} - 1\right) \tag{8}$$

where

$P_{dyn(a)}$ is the dynamic pressure on the fixed particle;

ρ_a is the density of the fixed particle;

ρ_o is the density of the fluid at rest;

$\gamma = 7$;

B is the term related to the density fluctuations of the fluid.

In hydrostatic cases, it is suggested employment of the modified pressure concept (Batchelor, 2000).

A simple boundary treatment in SPH is the implementation of the collisions of particles against solid walls, considered as being well-defined planes. Figure 5 shows the initial and final positions, C_0 and C_f, of the centre of mass of a particle after successively colliding with two planes (A and B) in a numerical iteration (Fraga Filho, 2014). The point C_1 is the final position that would be achieved by the particle's mass centre if there were no walls delimiting the field.

An analogy to molecular dynamics is also used in the boundary treatment in SPH. The solid boundary treatment uses a row of frozen particles (virtual particles) located on the solid contour to produce a highly repulsive force acting on the particles close to the contour (Monaghan, 1994). This type of virtual particles is known as type I (located on the contour). Prevention of the moving solid particles penetrating into contours is performed by a repulsion

force (similar to the Lennard-Jones molecular force) that simulates the boundary conditions with zero normal velocity. In certain situations, virtual particles of type II can be located outside the contour (Liu & Liu, 2003). Figure 6 shows the use of both types of virtual particles, in order to simulate the solid contours.

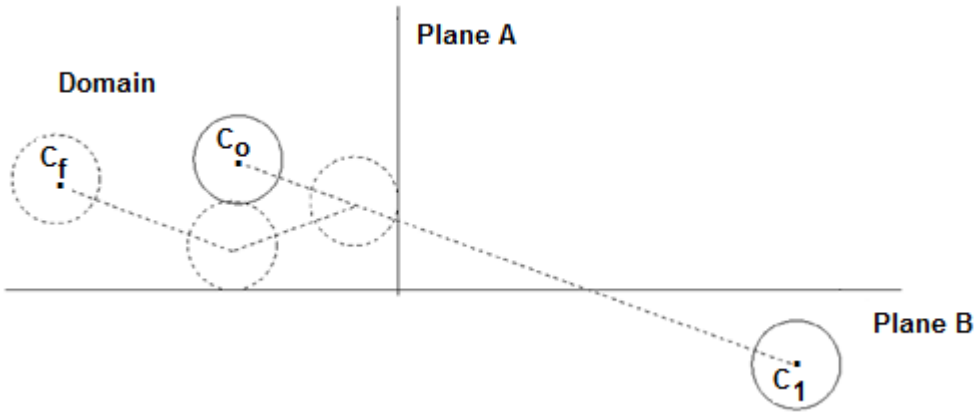

Figure 5. Collisions experienced by a particle in a time step.

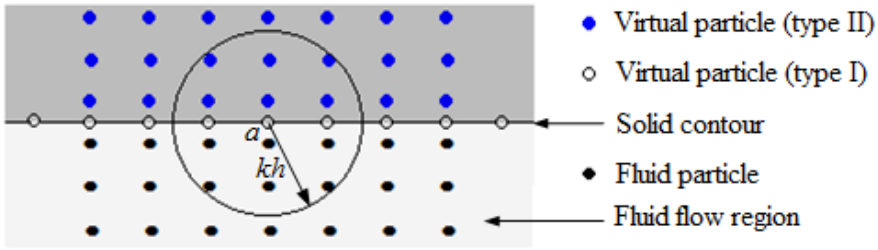

Figure 6. Schematic illustration of the solid contour region. Arrangement of the virtual particles of type I (line on the contour) and of the virtual particles of type II (in an extended area beyond the domain).

A broader presentation of the boundary conditions employed in SPH method may be encountered in (Fraga Filho, 2014).

In regions near the boundaries, the reference particles do not have a full influence domain, which reduces the accuracy of the interpolations performed. This phenomenon is known as particle inconsistency. For consistency restoration, some workers have proposed the application of a correction factor, presented as the Corrected Smoothed Particle Method (CSPM) (Chen et al., 1999; Fraga Filho, 2014). Figure 7 shows the occurrence of kernel truncation.

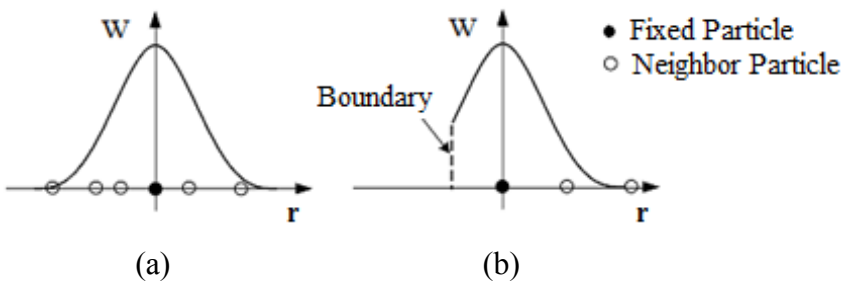

Figure 7. Influence domain in a polar coordinate system. (a) Complete and (b) incomplete.

3.1 SPH Approximations for Differential Equations in Fluid Mechanics and Heat Transfer

Modelling of fluid flows and energy transport is performed by the conservation (mass and energy) and momentum balance equations. The evolution of the field densities, velocities and energy is defined by Eqs. (9)–(11). Table 1 shows the conservation and momentum balance equations, according to the Lagrangian frame of reference, and their approximations by SPH to a viscous and incompressible fluid.

Table 1. Differential Equations and SPH Approximations

Differential Equation (Continuum)	SPH Approximation (Domain discretised by particles)	
Mass conservation: $\frac{d\rho}{dt} = -\rho \nabla . \mathbf{v}$	$\frac{d\rho_a}{dt} = \sum_{b=1}^{n} m_b \mathbf{v}_{ab} . \nabla W(\boldsymbol{X}_a - \boldsymbol{X}_b, h)$	(9)
Momentum balance: $\frac{d\mathbf{v}}{dt} = -\frac{\nabla P}{\rho} + \upsilon \nabla^2 \mathbf{v} + \mathbf{g}$	$\frac{d\mathbf{v}_a}{dt} = \sum_{b=1}^{n} m_b \left(\frac{P_a}{\rho_a^2} + \frac{P_b}{\rho_b^2} \right) \nabla W(\boldsymbol{X}_a - \boldsymbol{X}_b, h) + +2\upsilon_a \sum_{b=1}^{n} \frac{m_b}{\rho_b} \mathbf{v}_{ab} \frac{(\boldsymbol{X}_a - \boldsymbol{X}_b)}{\lvert \boldsymbol{X}_a - \boldsymbol{X}_b \rvert^2} . \nabla W(\boldsymbol{X}_a - \boldsymbol{X}_b, h) + \mathbf{g}$	(10)
Energy conservation: $\frac{de}{dt} = \frac{1}{\rho}(-P . \nabla \mathbf{v} + \varepsilon_v + \nabla . \mathbf{q} + q_H)$	$\frac{de_a}{dt} = \frac{1}{\rho} \left[-P_a \sum_{b=1}^{n} m_b \mathbf{v}_{ab} . \nabla W(\boldsymbol{X}_a - \boldsymbol{X}_b, h) + \varepsilon_v + +\nabla . \mathbf{q} + q_H \right]$	(11)

where:

$\mathbf{v}$ is the velocity;

$\mathbf{g}$ is the acceleration due to gravity;

υ is the kinematic fluid viscosity;

P is the pressure;

t is the time;

e is the specific internal energy;

ε_v is the energy dissipation per unit volume;

$\mathbf{q}$ is the conduction heat flux;

q_H is the heat generated by other sources per unit volume;

$\mathbf{v}_{ab} = \mathbf{v}_a - \mathbf{v}_b$;

a and b are subscripts that refer to fixed and neighbouring particles, respectively.

4 COMPUTER CODE

Figure 8 shows the flowchart of the computer code developed and implemented using FORTRAN programming language. The algorithm has been written for serial computation.

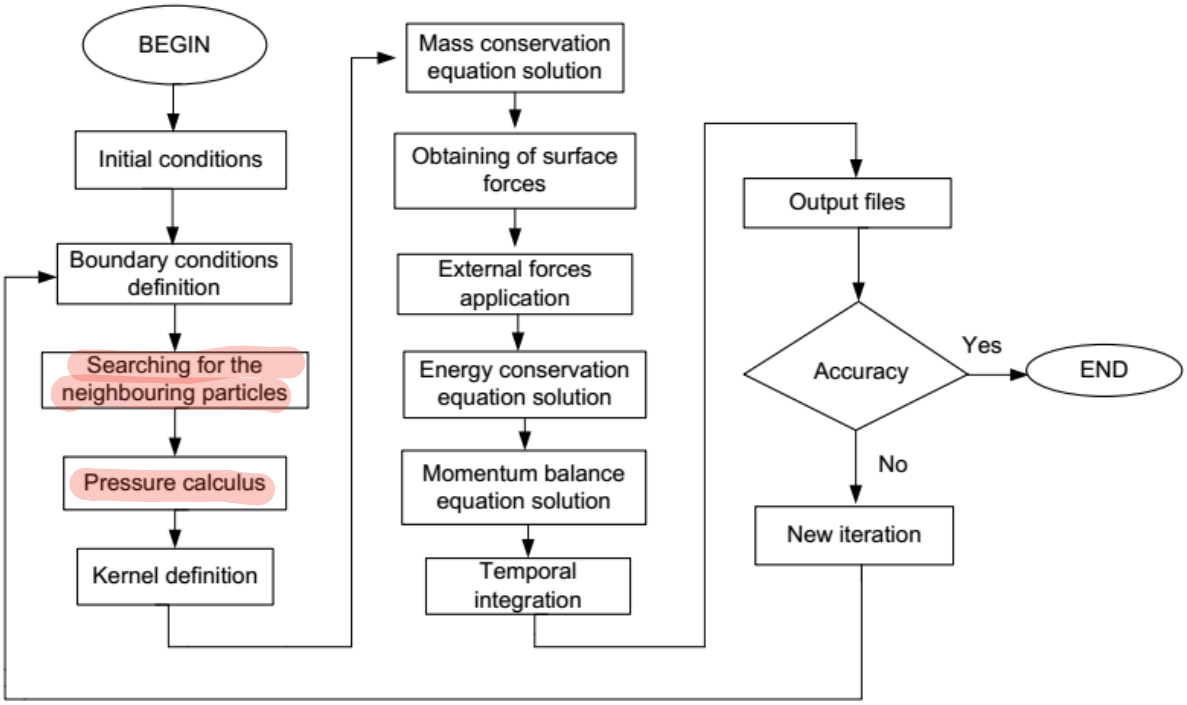

Figure 8. Algorithm implemented with all routines.

Below follows a brief presentation of the code and its routines.

1. Initial conditions: the initial positions, velocities, densities, temperatures, support radius and other fluid particles' physical properties are set to the beginning of the simulation.

2. Boundary conditions definition: the technique to be employed for the boundary treatment is defined.

3. Searching for the neighbouring particles: particles within the domain of influence of a reference particle may vary over time, and the search must be performed at each numerical iteration.

4. Pressure calculus: in this routine, updating of the pressure field acting on the particles is performed.

5. Kernel definition: smoothing function used in interpolations is chosen.

6. Mass conservation equation solution: the particles' density calculus for each particle is conducted from solution of Eq. (9).

7. Obtaining of surface forces: approximations to surface forces acting on the particles are obtained (the first two terms of Eq. (10), pressure and viscous forces, respectively).

8. External forces application: the last term on the right side of Equation (10) is the sum of all external forces. In the class of external forces (third term on the right side of the Eq. (10)) is

the gravity. Other forces can also be considered such as the repulsive forces exerted by the particles on the contours of fluid particles (Lennard-Jones forces) and free surface forces, if they exist in the studied problem.

9. Energy conservation equation solution: SPH approximations are employed for solution of Eq. (11).

10. Momentum balance equation solution: particles' accelerations field is obtained from solution of Eq. (10).

11. Temporal integration: prediction of the particles' properties to the next iteration. The Courant-Friedrichs-Lewy (CFL) stability criterion was applied in the time-step setting to ensure convergence of results (Courant et al., 1967).

12. Output files: these files are obtained at the end of each numerical iteration and, from their data, graphical representations of the fluid's physical properties are generated.

13. Accuracy: this routine verifies whether the desirable accuracy has been achieved or if a new iteration will have to be executed. In the latter case, we must return to step 2 (boundary conditions definition) and follow the remaining steps until a new verification of the accuracy of numerical results be performed.

In steps 6 and 7, the correction of the particles' physical properties (density and pressure gradient) located near the boundaries can be made using the Corrected Smoothed Particle Method (CSPM) (Chen et al., 1999; Liu and Liu, 2010).

5 CODE VALIDATION

Throughout the implementation, the numerical code was used for solution of some problems. Before the beginning of simulations, an examination of the physical phenomenon was carried out to select the routines to be used (Fig. 8 shows all available routines). From the numerical results analysis, made through comparisons with analytical and results reported in the literature, it has been possible to validate the code for application in studied cases. In this section, the set of problems, their results, and a discussion of their results are presented and discussed.

5.1 Heat Diffusion in a Homogeneous Flat Plate

In the absence of pressure fields, energy dissipation, heat sources and considering a material with a constant thermal conductivity, energy conservation equation is written as follows (in a thermal steady state):

$$\frac{\partial^2 T}{\partial x^2} + \frac{\partial^2 T}{\partial y^2} = 0 \tag{12}$$

The dimensions and boundaries of the plate are shown in Fig. 9. The whole domain has temperature T_0 equal to $0°C$, at the initial time; that is, the initial temperature is uniform. The prescribed boundary conditions (Dirichlet boundary conditions) have been imposed: $0°C$ at right, left and lower sides and $100°C$ at upper side of the plate.

The calculation of the Laplacian of temperature for each iteration was done explicitly, in a polar coordinate system, by solving the following equation:

$$\left(\frac{\partial^2 T_a}{\partial \mathrm{x}^2}+\frac{\partial^2 T_a}{\partial \mathrm{y}^2}\right)^m = 2\sum_{b=1}^{n}\frac{m_b}{\rho_b}\left[T\left(X_a\right)^m - T\left(X_b\right)^m\right].\frac{\partial W(r,h)}{\partial r}\frac{1}{r_{ab}} \tag{13}$$

where

m is the current time step, b is the subscript indicating each neighbouring particle of the fixed particle, which is denoted by the subscript a, n is the number of particles within the domain of influence, $r_{ab} = \left|\boldsymbol{X}_a - \boldsymbol{X}_b\right|$ is the distance between two particles, and r is the radial direction.

Pletcher et al. (2013) employed the technique of the separation of variables to obtain the solution by series for the temperature distribution in the flat plane. This solution has been used as a standard for comparison with the results obtained by SPH simulations.

In the defining of the boundaries, virtual particles of type I were fixed at the contours at a ratio of two virtual particles for each real particle and the temperatures of the sides of the plate were attributed to them. Virtual particles' properties were not subject to interpolations to predict their temperatures (Dirichlet boundary condition). The particles inside the domain had their temperatures initialized to 0 °C and the thermal diffusivity was defined as 1.0 m^2/s, which was held constant for all simulations. The influence domain ($\mathrm{k}h$) was defined as 2.5 $d\mathrm{x}$, which was invariable during simulations. The time step was 1.0 x 10^{-5} s.

Simulations were carried out starting from the transient until the steady state was reached. Different combinations of numbers of particles (50, 60, 70, 80, and 90 per side of the flat plate) and kernels have been used. Figure 9 shows the initial distribution of 50 × 50 particles in the domain (and the prescribed temperatures at the boundaries, attributed to the virtual particles) and the temperature distribution when the steady state was reached (t = 0.431 s).

For internal regions of the domain, the approximation of the Laplacian of the temperature by the SPH method gave results that were in agreement with the analytical solution.

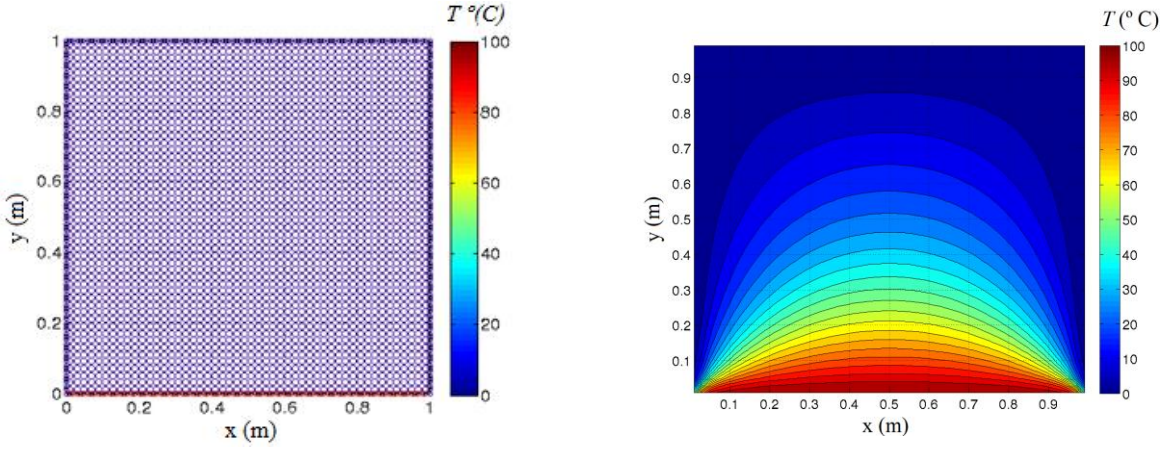

(a) (b)

Figure 9. (a) Initial distribution of 50 × 50 particles in the domain and the prescribed temperatures at the boundaries (attributed to the virtual particles). (b) Temperature distribution when the steady state has been reached (a cubic spline kernel was employed).

In all combinations of particle numbers and kernels, particle inconsistency has been seen in the regions near the boundaries, because kernel truncation correction has not been realized. The largest relative errors found in the steady state (obtained from the analysis of the differences between the analytical solution and the SPH numerical results) occurred in a few positions of the lower corners of the flat plate. The complete analysis of simulations results is in (Fraga Filho & Chacaltana, 2014, Fraga Filho, Pezzin & Chacaltana, 2014).

Figure 10 presents the algorithm implemented in a flowchart scheme (wherein the enabled routines in the computer program is shown).

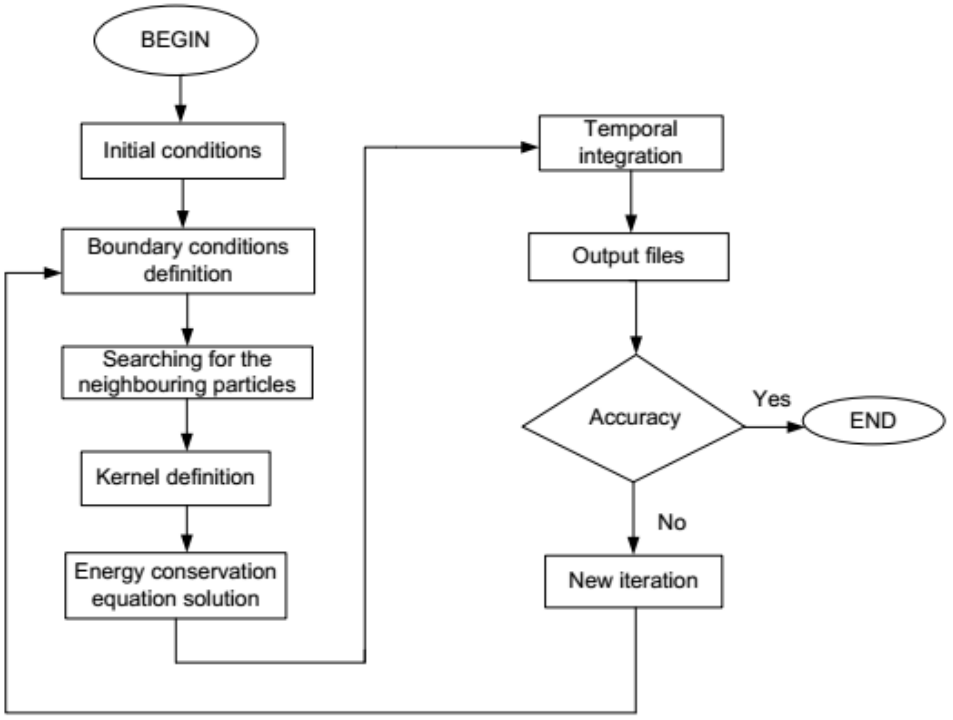

Figure 10. Algorithm implemented for diffusion in a homogeneous flat plane.

5.2 Still Fluid within an Immobile Reservoir

This is one of the first problems that must be understood and solved in Fluid Mechanics. There is a tank filled with an incompressible, uniform and isothermal fluid. The student must be able to understand the physical problem and, from there, apply the physical laws of mass conservation and momentum balance, and the concept of the modified pressure (Batchelor, 2000). Using this concept, the momentum balance equation (Eq. (10)) is rewritten as follows:

$$\frac{\mathrm{d}\mathbf{v}_a}{\mathrm{dt}} = \sum_{b=1}^{n} m_b \left(\frac{P_{\mathrm{mod}(a)}}{\rho_a^2} + \frac{P_{\mathrm{mod}(b)}}{\rho_b^2} \right) \nabla W\left(\boldsymbol{X}_a - \boldsymbol{X}_b, h\right) + \\ +2\upsilon_a \sum_{b=1}^{n} \frac{m_b}{\rho_b} \mathbf{v}_{ab} \frac{(\boldsymbol{X}_a - \boldsymbol{X}_b)}{\left|\boldsymbol{X}_a - \boldsymbol{X}_b\right|^2} . \nabla W\left(\boldsymbol{X}_a - \boldsymbol{X}_b, h\right) \tag{14}$$

where $P_{\mathrm{mod}(a)}$ and $P_{\mathrm{mod}(b)}$ are the modified pressures on the fixed particle and the neighbouring particle, respectively.

Figure 11 shows the regular initial arrangement of particles in the reservoir.

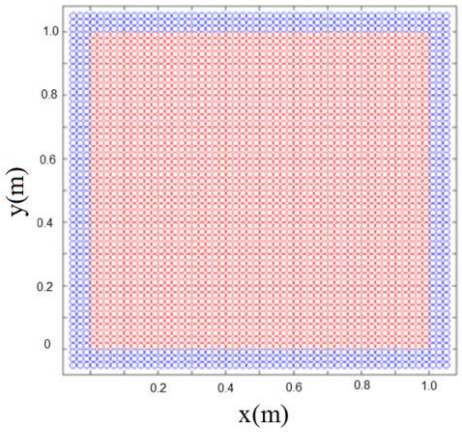

Figure 11. Initial distribution of fluid particles (red) and virtual particles (blue). The latter are in an expanded region of the domain.

In hydrostatic case, modified pressure on all particles is null (Fraga Filho & Chacaltana, 2015). Figure 12 (a) presents the final results (in which the hydrostatic equilibrium has been maintained). Figure 12 (b) presents the constant hydrostatic pressure field, in the colour scale graph.

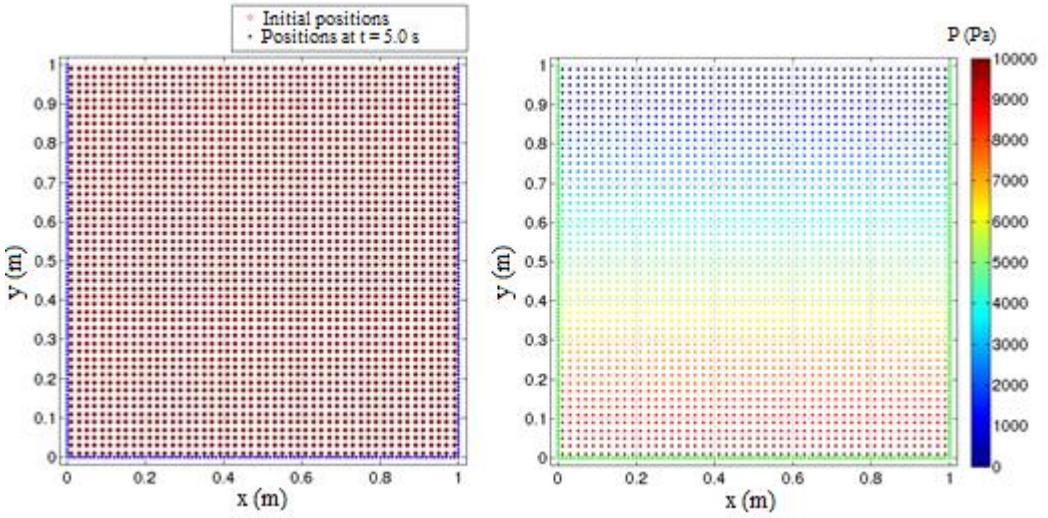

Figure 12. (a) Positions of the particles within the reservoir, time invariant. (b) Hydrostatic pressure field on the particles, constant with time.

After starting the simulation, at the time instance 5.0 s, the coincidence of the positions of the centers of mass at that moment and their initial positions was verified, in agreement with the analytical solution.

The flowchart, in Fig. 13, shows the enabled routines in the computer program used for solution of the hydrostatic problem.

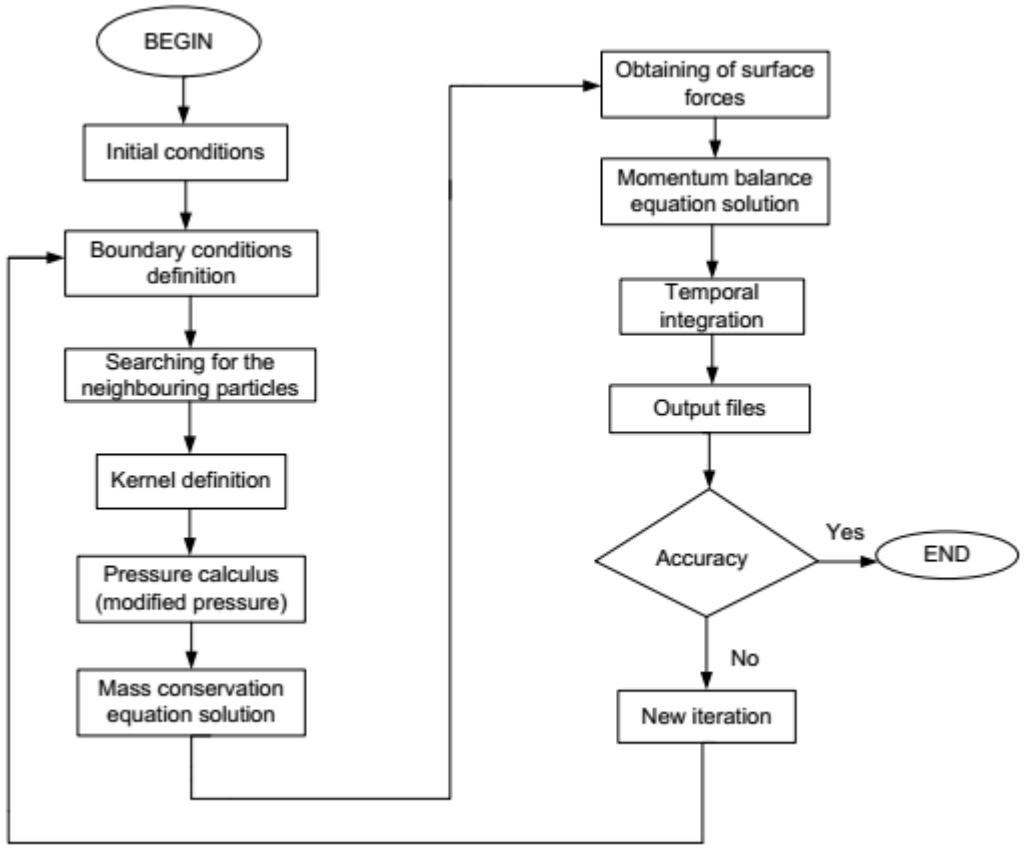

Figure 13. Flowchart of the numerical code for the reservoir problem containing an incompressible fluid and open to the atmosphere.

5.3 Dam Breaking

This is a classic problem of fluid dynamics. Dam breaking studies are of great importance in engineering, being related to the prevention of accidents, which can cause serious environmental consequences and also damage to inhabitants located in the vicinity.

The fluid is considered incompressible, uniform and isothermal; the Navier-Stokes equations, mass conservation and momentum balance (Eqs. (9) and (10)), must be solved.

Figure 14 shows the initial distribution of particles' centers of mass and the evolution of the wave until the time 1.00 s.

The numerical results showed good agreement with experimental results reported in the literature. A detailed description of simulations performed and all results obtained can be found in Fraga Filho (2014).

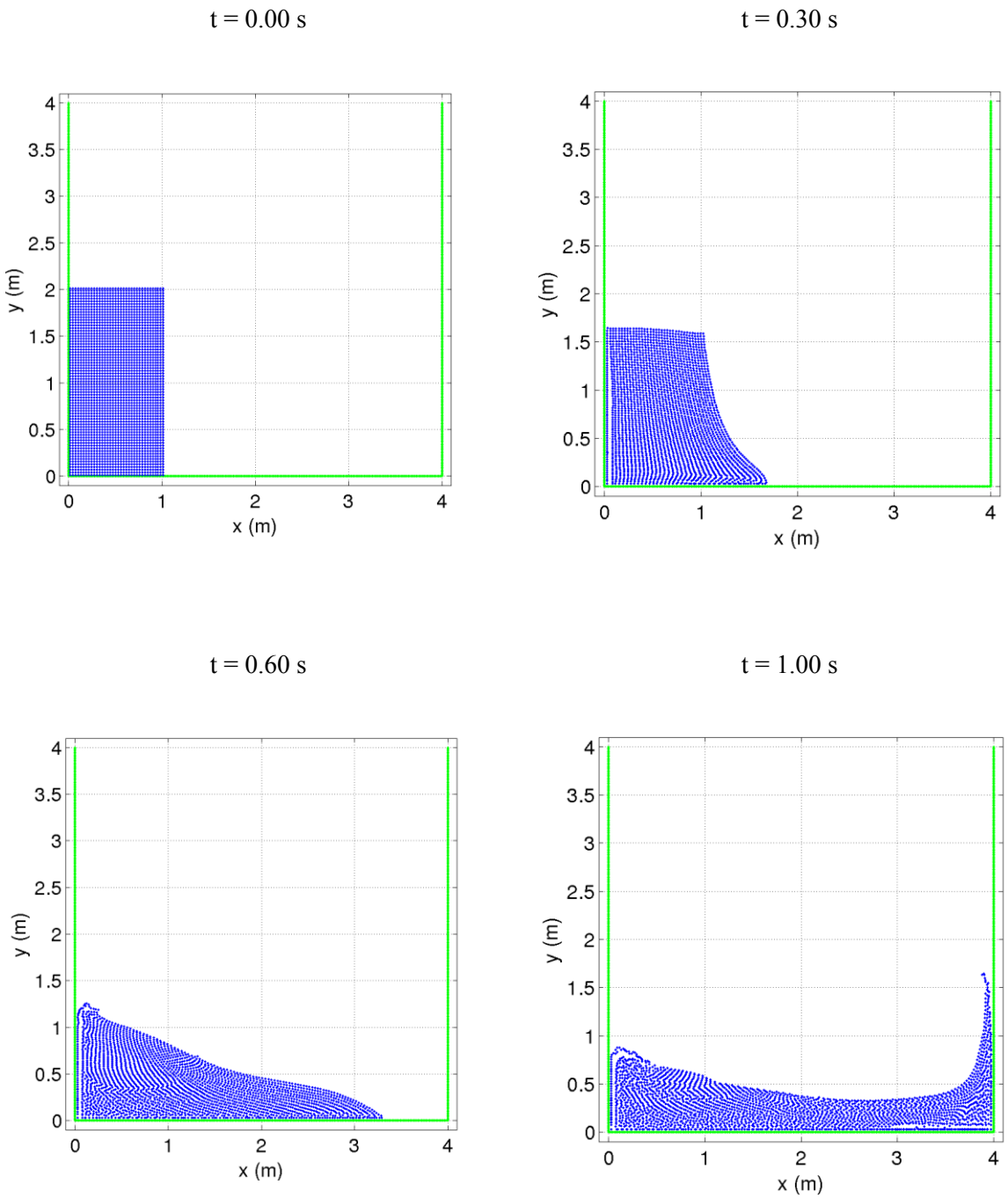

Figure 14. Dam breaking evolution.

In Figure 15, a flowchart shows the numerical code implemented for solution of dam break problem.

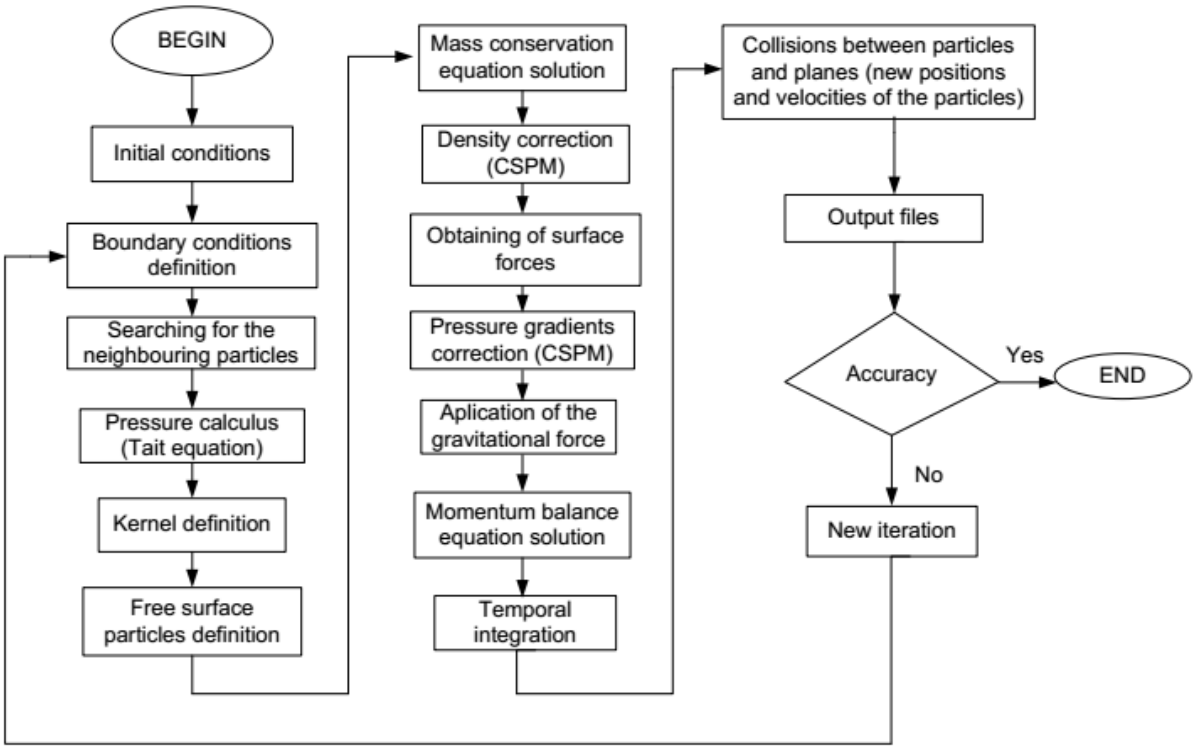

Figure 15. Flowchart of the numerical code implemented for dam breaking.

6 CONCLUSIONS

The Lagrangian approach is still little used in engineering studies. However, due to the advances in computer processing techniques, there has been an increase in the applications of the Lagrangian Meshless SPH Method in Computational Fluid Dynamics (CFD) courses. SPH is a problem-solving alternative that has advantages compared to traditional methods using meshes, e.g. better visualisation of the spatio-temporal evolution of the flow, and a lower computational cost in the study of complex geometries with topological changes or free surfaces beyond the control of undesirable numerical diffusion. From the graphical analysis of the results, by viewing the properties of particles (which may be fields of positions, velocities, accelerations, pressures, among others) a better understanding of the phenomenon that occurs is reached.

The numerical code developed has been employed in the simulations of some phenomena: diffusion in a flat plate, still fluid inside an immobile reservoir and dam breaking. In code validation, numerical results obtained showed a good agreement with the analytical and experimental results reported in the literature.

The code implemented, and presented in this work, is a valuable tool for CFD education in engineering courses.

ACKNOWLEDGEMENTS

The author would like to thank for a grant provided by the Research Support Foundation of the State of Espírito Santo (FAPES) (no. 46352724/2009). I also thank Prof. Dr Julio Tomas Aquije Chacaltana and Prof. Dr Maxsuel Marcos Rocha Pereira for their comments and suggestions.

REFERENCES

Batchelor, G.K., 2000. *An Introduction to Fluid Dynamics*. Cambridge University Press, 3rd edition, Cambridge, UK.

Chen, J. K., Beraun, J.E. & Carney, T. C., 1999. A Corrective Smoothed Particle Method for Boundary Value Problems in Heat Conduction. *International Journal for Numerical Methods in Engineering*, 46: 231-252.

Courant R., Friedrichs K., & Lewy H., 1967. On the partial difference equations of mathematical physics. *IBM Journal*, 11:215-234.

Crespo A.J.C., Dominguez J.M., Barreiro A., Gomez-Gesteira., & Rogers B.D., 2011. GPUs, a new tool of acceleration in CFD: efficiency and reliability on Smoothed Particle Hydrodynamics methods. *PLoS ONE* 6 (6).

Fox, R.W., & McDonald, A.T., 1998. Introdução à Dinâmica dos Fluidos, 3ª Edição, Rio de Janeiro: Editora Guanabara.

Fraga Filho, C.A.D., 2014. Estudo da Fase Gravitacional-inercial do Espalhamento de Óleo em Mar Calmo empregando o Método Lagrangiano de Partículas Smoothed Particle Hydrodynamics. PhD Thesis, Federal University of Espírito Santo, Brazil. Available at: http://cfd.mace.manchester.ac.uk/sph/SPH_PhDs/2014/Carlos_Alberto_DUTRA_FRAGA_FILHO_PhD_Thesis_2014.pdf [Accessed: 20 March 2016].

Fraga Filho, C.A.D., & Chacaltana, J.T.A., 2014. Numerical Study of Heat Diffusion Employing the Lagrangian Smoothed Particle Hydrodynamics Method: an Analysis of the Applicability of the Laplacian Operator and the Influence of the Boundaries on the Solution. *International Review on Modelling and Simulations (I.RE.MO.S.)*, 2014, vol. 7, N. 6, pp. 994-1002.

Fraga Filho, C.A.D., Pezzin D.F., & Chacaltana, J.T.A., 2014. A numerical study of heat diffusion using the Lagrangian particle SPH method and the Eulerian Finite-Volume method: analysis of convergence, consistency and computational cost. *Proceedings of the Thirteenth International Conference on Simulation and Experiments in Heat and Mass Transfer (Heat Transfer XIII), WIT Press*, pp. 15-26, UK (2014).

Fraga Filho, C.A.D., & Chacaltana, J.T.A., 2015. Study of fluid flows using Smoothed Particle Hydrodynamics: the modified pressure concept applied to quiescent fluid and dam breaking. *Proceedings of the XXXVI Iberian Latin-American Congress on Computational Methods in Engineering*, Rio de Janeiro, Brazil (2015). Available at: https://ssl4799.websiteseguro.com/swge5/PROCEEDINGS/PDF/CILAMCE2015-0071.pdf [Acessed: 21 August 2016]

Gesteira, M. G., Rogers, B. D., Dalrymple R. A., & Crespo A. J. C., Narayanaswamy, 2010. User Guide for SPHysics Code. Available at: https://wiki.manchester.ac.uk/sphysics/index.php?title=Special:UserLogin&returnto=SPHYSICS+2D+Download+v2.2 [Accessed: 27 June 2016].

Liu · M. B., & G. R. Liu, 2003. Smoothed Particle Hydrodynamic, A Meshfree Particle Method. World Scientific Publishing Co. Pte. Ltd.

Liu · M.B., & G.R. Liu, 2010. Smoothed Particle Hydrodynamics (SPH): an Overview and Recent Developments. *Arch. Comput. Methods Eng*., 17: 25-76.

Lucy L.B., 1977. Numerical approach to testing the fission hypothesis. *Astronomical Journal*, 82:1013-1024.

Monaghan J. J., 1994. Simulating free surface flows with SPH. *J. Comput. Phys*.,110 (2):399-406.

Morris, J. P., Fox, P. J., & Zhu, Y., 1977. Modeling Low Reynolds Number Incompressible Flows Using SPH. *Journal of Computational Physics*, 136: 214-226.

Pletcher, R.H., Tanehill, J.C., & Anderson D.A., 1997. *Computational Fluid Mechanics and Heat Transfer*. Taylor and Francis, 2nd edition, London, UK.